APPENDIX 1

CORRELATION OF DOUBLE SIDE BAND SIGNALS

Consider the signals from the antenna 1 (Fig A1.1) of amplitudes A_{1+} and A_{1-}, and phases φ_{1+} and φ_{1-} respectively with respect to that of the local oscillator signal (frequency ω_o) having the frequencies ω_+ and ω_- respectively, given by:

$$\omega_{\pm} = \omega_o \pm \omega_{if}$$

Note that both these components of the input signal produce on heterodying with local oscillator signal at ω_o, the same IF frequency, ω_{if}. That is, the input signal from Antenna 1 may be written as:

$$A_{1c} = A_{1+} \cos(\omega_+ t + \varphi_{1+}) + A_{1-} \cos(\omega_- t + \varphi_{1-}) \quad \ldots\ldots(A1.1)$$

Similarly, the signal from Antenna 2, may be written as:

$$A_{2c} = A_{2+} \cos(\omega_+ t + \varphi_{2+}) + A_{2-} \cos(\omega_- t + \varphi_{2-}) \quad \ldots\ldots(A1.2)$$

It may be easily shown that these signals given in Equations (A1.1) and (A1.2) on heterodyning (Fig A1.1) with the local oscillator signal at ω_o given by $A_o \cos\omega_o t$ and passing the resulting signals through low pass filters give the following signals:

$$S_1 = \frac{A_o A_{1+}}{2} \cos(\omega_{if} t + \varphi_{1+}) + \frac{A_o A_{1-}}{2} \cos(\omega_{if} t - \varphi_{1-}) \ldots(A1.4)$$

$$S_2 = \frac{A_o A_{2+}}{2} \cos(\omega_{if} t + \varphi_{2+}) + \frac{A_o A_{2-}}{2} \cos(\omega_{if} t - \varphi_{2-}) \ldots(A1.5)$$

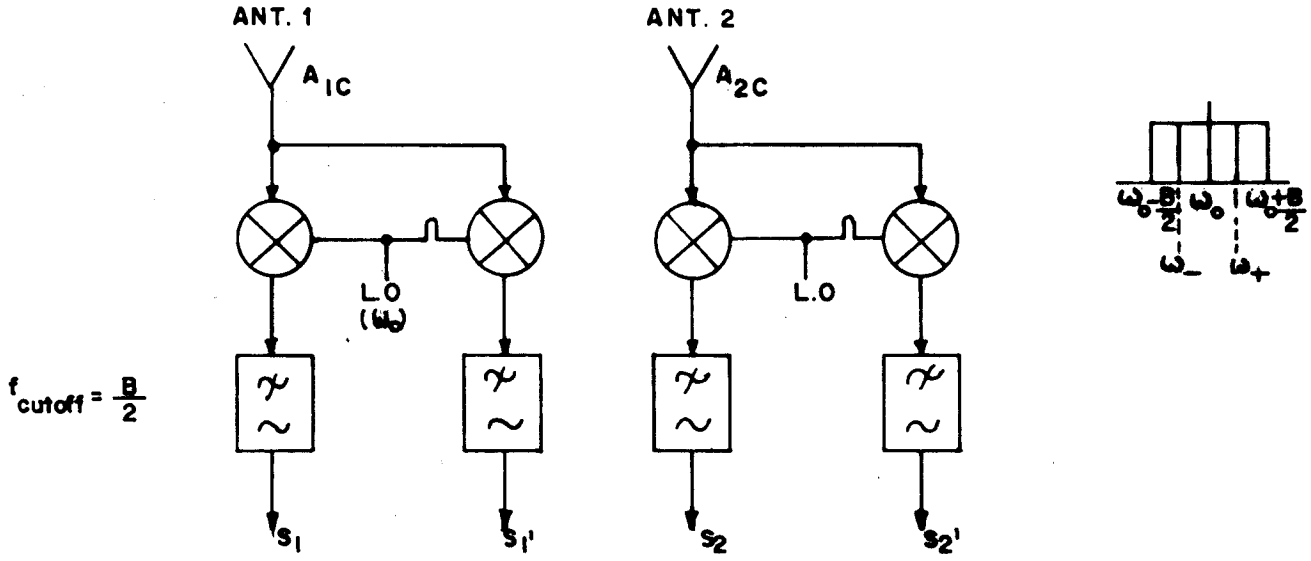

FIG. A1.1(A) DSB SIGNAL GENERATION.

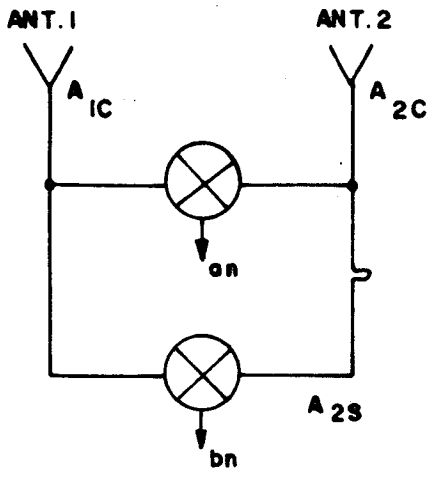

FIG A1.1(B) CORRELATION OF RF SIGNALS.

Further, when the signals given in equation (A1.1) and (A1.2) are heterodyned with a local oscillator shifted by 90^{o} in phase, and passed through the low-pass filters, give the following output signals:

$$S_1' = \frac{A_o A_{1+}}{2} \text{Sin } (\omega_{if} t + \varphi_{1+}) - \frac{A_o A_{1-}}{2} \text{ Sin } (\omega_{if} t - \varphi_{1-}) \ldots (A1.6)$$

$$S_2' = \frac{A_o A_{2+}}{2} \text{Sin } (\omega_{if} t + \varphi_{2+}) - \frac{A_o A_{2-}}{2} \text{ Sin } (\omega_{if} t - \varphi_{2-}) \ldots (A1.7)$$

Correlating the output signals S_1 and S_2, that is by multiplying the signal S_1 with S_2 and integrating the product over a sufficient length of time, yields the following signal:

$$\overline{S_1 S_2} = \frac{A_o^2}{8} A_{1+} A_{2+} \text{ Cos } (\varphi_{1+} - \varphi_{2+}) + \frac{A_o^2}{8} A_{1-} A_{2-} \text{ Cos } (\varphi_{1-} - \varphi_{2-})$$

$$+ \frac{A_o^2}{8} A_{1+} A_{2-} \text{ Cos } (\varphi_{1+} + \varphi_{2-}) + \frac{A_o^2}{8} A_{1-} A_{2+} \text{ Cos } (\varphi_{1-} - \varphi_{2+})$$

$$\ldots\ldots (A1.8)$$

Similarly S_1' with S_2' gives

$$\overline{S_1' S_2'} = \frac{A_o^2}{8} A_{1+} A_{2+} \text{ Cos } (\varphi_{1+} - \varphi_{2+}) + \frac{A_o^2}{8} A_{1-} A_{2-} \text{ Cos } (\varphi_{1-} - \varphi_{2-})$$

$$- \frac{A_o^2}{8} A_{1+} A_{2-} \text{ Cos } (\varphi_{1+} + \varphi_{2-}) - \frac{A_o^2}{8} A_{1-} A_{2+} \text{ Cos } (\varphi_{1-} + \varphi_{2+})$$

$$\ldots\ldots (A1.9)$$

Adding the outputs of the above mentioned correlators, the following signal is obtained:

$$S_c = \overline{S_1 S_2} + \overline{S_1' S_2'}$$

$$= \frac{A_o^2}{4} A_{1+}A_{2+} \cos(\varphi_{1+} - \varphi_{2+}) + \frac{A_o^2}{4} A_{1-}A_{2-} \cos(\varphi_{1-} - \varphi_{2-}) \quad \ldots\ldots(A1.10)$$

It is easy to show that if the signals given by equation (A1.1) and (A1.2) are correlated at the r.f. level itself, the following output would be obtained giving the cosine correlation:

$$a_n = A_{1+}A_{2+} \cos(\varphi_{1+} - \varphi_{2+}) + A_{1-}A_{2-} \cos(\varphi_{1-} - \varphi_{2-}) \ldots(A1.11)$$

Note that from the above equations (A1.10) and (A1.11),

$$a_n = S_c = \overline{S_1 S_2} + \overline{S_1' S_2'} \quad \ldots\ldots(A1.12)$$

Similarly, it may be established that the sine correlation, b_n, given by:

$$b_n = A_{1+} A_{2+} \sin(\varphi_{1+} - \varphi_{2+}) + A_{1-}A_{2-} \sin(\varphi_{1-} - \varphi_{2-}) \ldots(A1.13)$$

is the difference of the two correlators outputs $\overline{S_2 S_1'}$ and $\overline{S_1 S_2'}$.

That is,

$$b_n = \overline{S_2 S_1'} - \overline{S_1 S_2'} \qquad \text{.....(A1.14)}$$

Hence, a_n and b_n may be obtained as given in the block diagram Fig 3.5.

APPENDIX 2

Derivation of Correlation Coefficient from the Counter Value

The Correlation Coefficient, ρ_c , of a one-bit correlator circuit is given by Weinreb (1963).

$$\rho_c = \frac{K_c - K_a}{K} = \frac{2K_c - K}{K} = \frac{K - 2K_a}{K} \quad \ldots\ldots\ldots (A2.1)$$

where K_c, number of coincidences

K_a, number of anticoincidences and

$K = K_c + K_a$, total number of samples.

Therefore, the correlation coefficient, ρ_c , may be determined by observing K_c and K, using an EXNOR gate or by observing K_a and K, using an EXOR gate.

Consider the sampling rate of the system such that n samples are obtained in a given pre-integration time. Since two correlators are used for Cosine and Sine correlations, the counter should be capable of counting 2n samples without overflow.

For the Cosine Correlation, two EXNOR gates are used to implement the products S_1S_2 and $S_1'S_2'$. Let the counts of these two gates be n_{cc} and n_{cc}'. From equation(A2.1) the normalised correlation coefficient

can be written as:

$$a_n = \frac{1}{2}\left[\frac{2n_{cc}-n}{n} + \frac{2n_{cc}'-n}{n}\right]$$

$$= \frac{(n_{cc} + n_{cc}') - n}{n} \qquad \ldots\ldots(A2.2)$$

Similarly the Sine correlation, b_n, can be expressed as:

$$b_n = \frac{(n_{sc} + n_{sa}') - n}{n} \qquad \ldots\ldots(A2.3)$$

where n_{sc} is number of coincidences of an EXNOR gate used for $S_1'S_2$ and n_{sa}' is number of anticoincidences of an EXOR gate used for $S_2'S_1$.

To facilitate further processing, the correlation coefficients are expressed in 2'S complement form as given below:

$$\left.\begin{aligned} a_n &= \frac{(n_{cc} + n_{cc}') - n}{n} \quad \text{for } (n_{cc} + n_{cc}') > n \\ &\quad \frac{(n_{cc} + n_{cc}') + n}{n} \quad \text{for } (n_{cc} + n_{cc}') < n \\ b_n &= \frac{(n_{sc} + n_{sa}') - n}{n} \quad \text{for } (n_{sc} + n_{sa}') > n \\ &\quad \frac{(n_{sc} + n_{sa}') + n}{n} \quad \text{for } (n_{sc} + n_{sa}') < n \end{aligned}\right\} \qquad (A2.4)$$

Note that as n is half the maximum counter value, the subtraction or the addition of n required in the above set of equations amounts to changing only the most significant bit of the counter value. The same is verified as given in Tables (A2.1) to (A2.3).

TABLE A2.1

CONVERING COUNTER VALUES TO CORRELATION VALUES

Correlation Value	Counter Value as fraction of total No. of samples	
	with EXNOR gate	with EXOR gate
1	1	0
0	1/2	1/2
-1	0	1

TABLE A2.2

Extreme conditions of correlators

in

Cosine Correlation

COR. 1 S_1S_2	COR. 2 $S_1'S_2'$	SUM SUM	expected 2'S COMP VALUE	Counter Value with EXNOR gates $(S_1 \oplus S_2) + (S_1' \oplus S_2')$	
1	1	2	0111	2	1111
1	0	1	0100	1½	1100
1	-1	0	0000	1	1000
0	1	1	0100	1½	1100
0	0	0	0000	1	1000
0	-1	-1	1100	½	0100
-1	1	0	0000	1	1000
-1	0	-1	1100	½	0100
-1	-1	-2	1000	0	0000

TABLE A2.3

Extreme conditions of correlators

in

Sine Correlation

COR. 1 S_2S_1'	COR. 2 S_1S_2'	Difference $S_2S_1' - S_1S_2'$		Counter value $\overline{(S_2 \oplus S_1')} + (S_1 \oplus S_2')$	
1	1	0	0000	1	1000
1	0	1	0100	1½	1100
1	-1	2	0111	2	1111
0	1	-1	1100	½	0100
0	0	0	0000	1	1000
0	-1	1	0100	1½	1100
-1	1	-2	1000	0	0000
-1	0	-1	1100	½	0100
-1	-1	0	0000	1	1000

APPENDIX - 3

Determination of brightness temperature from the measured antenna temperature

The complex antenna temperature, T_a, of a correlation telescope in terms of the brightness temperature distribution T_B (l,m) and the complex effective area A (l,m) is given by (Christiansen, 1969).

$$T_a = \lambda^{-2} \int_{4\pi} T_B (l,m) \quad A(l,m) \quad d\Omega \qquad (A3.1)$$

The correlation telescope effective area is given by:

$$A(l,m) = |A(l,m)| \exp j\psi \qquad (A3.2)$$

$$|A(l,m)| = 2 \left[A_1 (l,m) \; A_2 (l,m)\right]^{1/2} \qquad (A3.3)$$

where A_1 and A_2 are the effective areas of the two components and ψ= the phase difference of the signals arriving at the two antennas. For an interferometer whose electrical centres of the component antennas are separated by u wavelengths in the x direction and by v wavelengths in the y direction,

$$\psi = 2\pi (ul + vm) \qquad (A3.4)$$

$$\text{Since } d\Omega = \left[\frac{dl\, dm}{1-l^2-m^2}\right]^{1/2}, \text{ Eq. (A3.1)}$$

be written as

$$Ta\ (u,v) = \iint_{-\infty}^{+\infty} \frac{T_B\ (l,m)\ |\ A(l,m)|}{\lambda^2\ (1-l^2-m^2)^{1/2}} \exp \left\{j2\pi(ul+vm)\right\} \quad dldm \qquad \ldots.(A3.5)$$

This is a Fourier integral equation and hence

a Fourier pair of functions is given by

$$Ta\ (u,v) \quad \underline{FT} \quad \frac{T_B\ (l,m)\ |\ A(l,m)|}{\lambda^2\ (1-l^2-m^2)^{1/2}} \qquad \ldots\ldots\ldots \quad (A3.6)$$

Thus, a fixed spacing interferometer measures one Fourier component of the weighted brightness distribution. The required brightness distribution can be determined from the inverse Fourier transform of the correlation temperature T_a, which can be written as

$$\frac{T_B(l,m)\ |\ A(l,m)|}{\lambda^2(1-l^2-m^2)^{1/2}} = \iint_{-\infty}^{+\infty} Ta\ (u,v)\ \exp\ \left\{-j2\pi(ul+um)\right\}\ dudv \qquad \ldots\ldots(A3.7)$$

This is a fundamental equation of aperture synthesis. Thus brightness temperature can be determined from the measured antenna temperature of the correlation telescope with various spacings.

If the synthesis spacings (u, v) are chosen with regular intervals du and dv in the u and v directions respectively, then the equation (A3.7) can be replaced by a series. For simplicity LHS of equation (4A.7) is replaced by $T_{map}\ (l,m)$ and is given by

$$Tmap\ (l,m) = \sum_{-u}^{u} \sum_{-v}^{v} Ta(u,v)\ \exp\ \left\{-j2\pi(ul+vm)\right\} \qquad \ldots A3.8$$

The brightness temperature distribution $T_B\ (l,m)$

and the envelope pattern $|A(l,m)|$ are both real functions. The Fourier transform of real function is a Hermitian function, i.e., the real part of T_a is even and the imaginary part of T_a is odd. In other words,

$$T_a\ (-u, -v) = T_a^*\ (u,v) \quad \text{.....(A3.9)}$$

This means that if $T_a\ (u,v)$ is known, there is no need to measure $T_a\ (-u, -v)$ or in other words, only two of the quadrants in the u,v plane need be explored.

Denoting the real part and imaginary part of T_a by a_n and b_n, respectively, equation (A3.9) can be written as:

$$\text{Tmap}\ (l,m) = \sum_{-u}^{u} \sum_{-v}^{v} (an+jbn)\ \exp\left\{-j2\pi\ (ul+vm)\right\} \quad \text{..(A3.10)}$$

In one-dimensional synthesis which is presently employed, the equation reduces to

$$\text{Tmap}\ (m) = \sum_{-v}^{v} (a_n + jbn)\ \exp\left\{-j2\pi\ vm\right\} \quad \text{....(A3.11)}$$

Since $(a_n + jb_n)$ is a Hermitian quantity, as

already mentioned, its Fourier Transform is real. The equation (A3.11) can be thus written with positive values of v in the 2 measured quadrants of u, v plane as:

$$\text{Tmap}\ (m) = 2 \sum_{o}^{+V} \text{Re}\left[(a_n + j\, b_n) \exp\ (-j\ 2\Pi\ vm)\right] \quad \ldots.(A3\text{-}12)$$

$$\text{Tmap}\ (m) \propto \sum_{n=o}^{N} (a_n \text{ Cos } 2\Pi\ V_n\ m + b_n \text{ Sin } 2\Pi\ V_n\ m) \quad \ldots.(A3.13)$$

APPENDIX -4

DERIVATION OF PHASE CORRECTION EQUATION

Let an', bn' be the measured Cosine and Sine correlation coefficients and let an, bh are true Cosine and Sine correlation coefficients. True Correlation Coefficients are obtained by phase rotation of the measured Correlation Coefficients. The derivation of the equations are given below:

Case 1: + ($0^\circ < \Delta\psi < 179^\circ$)

$$\begin{vmatrix} a_n \\ b_n \end{vmatrix} = \begin{vmatrix} \text{Cos}\,(-\Delta\psi) & \text{Cos}\,(90-\Delta\psi) \\ \text{Cos}-(90+\Delta\psi) & \text{Cos}\,(-\Delta\psi) \end{vmatrix} \begin{vmatrix} a_n' \\ b_n' \end{vmatrix}$$

$$= \begin{vmatrix} \text{Cos}\,\Delta\psi & \text{Sin}\,\Delta\psi \\ -\text{Sin}\,\Delta\psi & \text{Cos}\,\Delta\psi \end{vmatrix} \begin{vmatrix} a_n' \\ b_n' \end{vmatrix}$$

i.e.

$$a_n = a_n' \text{ Cos } \Delta\psi + b_n' \text{ Sin } \Delta\psi \quad \cdots\cdots (A4.1)$$

$$b_n = b_n' \text{ Cos } \Delta\psi - a_n' \text{ Sin } \Delta\psi$$

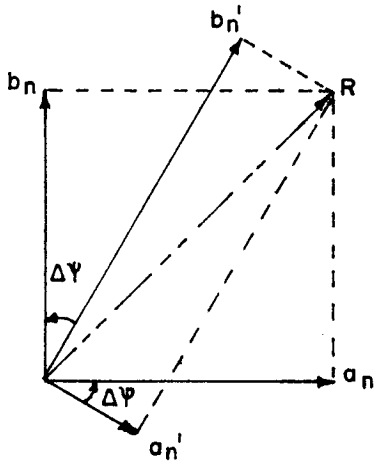

Case 2: $-\Delta\psi$ ($180^\circ < \Delta\psi < 359^\circ$)

$$\begin{vmatrix} a_n \\ b_n \end{vmatrix} = \begin{vmatrix} \text{Cos}\,\Delta\psi & \text{Cos}\,(90+\Delta\psi) \\ \text{Cos}-(90-\Delta\psi) & \text{Cos}\,\Delta\psi \end{vmatrix} \begin{vmatrix} a_n' \\ b_n' \end{vmatrix}$$

$$= \begin{vmatrix} \text{Cos}\,\Delta\psi & -\text{Sin}\,\Delta\psi \\ \text{Sin}\,\Delta\psi & \text{Cos}\,\Delta\psi \end{vmatrix} \begin{vmatrix} a_n' \\ b_n' \end{vmatrix}$$

i.e.

$$a_n = a_n' \text{ Cos } \Delta\psi - b_n' \text{ Sin } \Delta\psi \quad \cdots\cdots (A4.2)$$

$$b_n = b_n' \text{ Cos } \Delta\psi + a_n' \text{ Sin } \Delta\psi$$

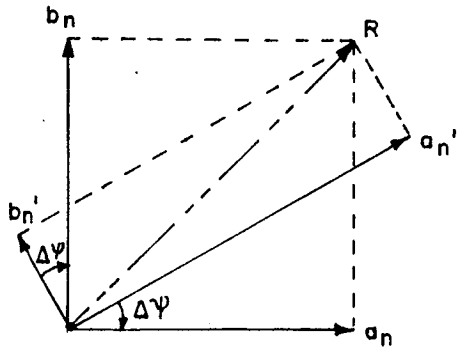

APPENDIX - 5

DETAILS OF THE MICROPROCESSOR, RCA 1802

Fig. A5.1(a) shows the block schematic of the microprocessor and Fig. A5.1(b) its internal architecture of CDP 1802 and Fig. A5.1(c) shows the typical computer system. The microprocessor architecture is based on a register array comprising sixteen general purpose (16 bit) scratch pad registers. Each scratch pad register R is designated by a 4 bit binary code. Three 4 bit registers labelled N, P and X hold the 4 bit binary codes that are used to select the 16 bit scratch pad registers. The 16 bits contained in a selected scratch pad can be used in several ways. Considered as two bytes, they may be sequentially placed on the eight external memory address lines for memory R/W operations. Either byte can also be gated to the 8 bit data bus for subsequent transfer to the D register. The 16 bit value in the A register can also be incremented or decremented by 1 and returned to a selected scratch pad register, so as to use this as a counter. The 8 bit ALU performs arithmetic and logical operations. A sign signal bit register DF (data Flag) is used in shift and arithmetic operations. 15 input/output lines are provided for expanding the computer system as shown in Fig. A5.1(b). User manual MPM-201A gives the details of instruction sets and typical applications.

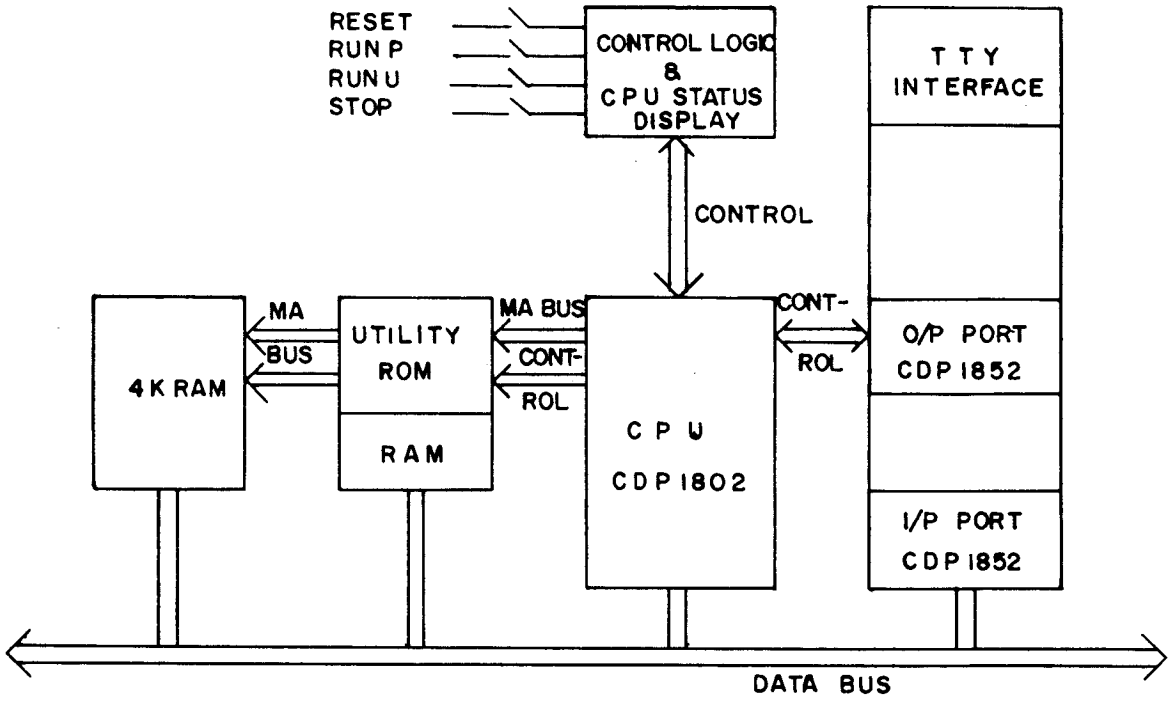

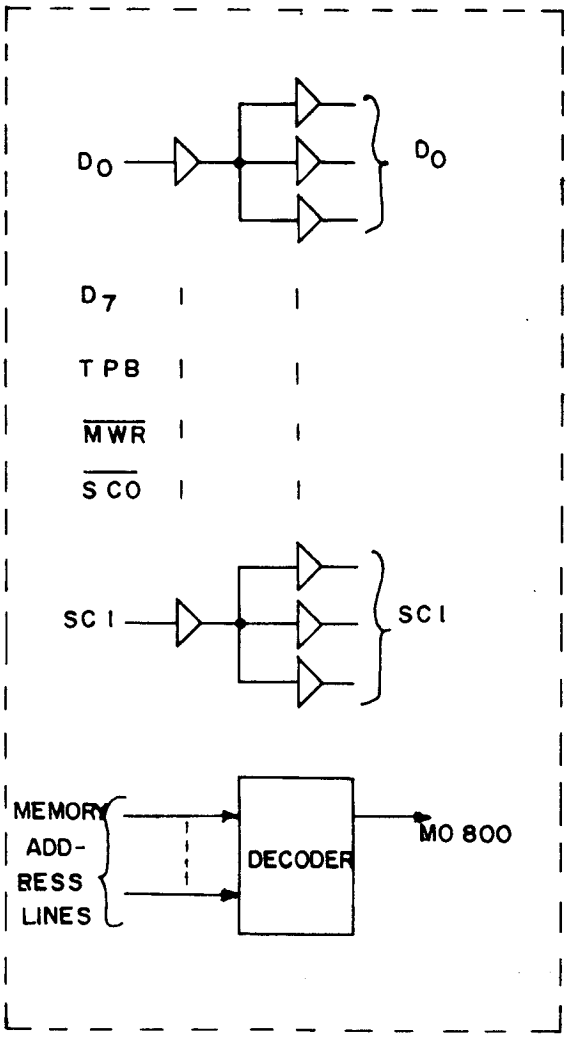

FIG. A5.1.(a). BLOCK SCHEMATIC OF MICROPROCESSOR.

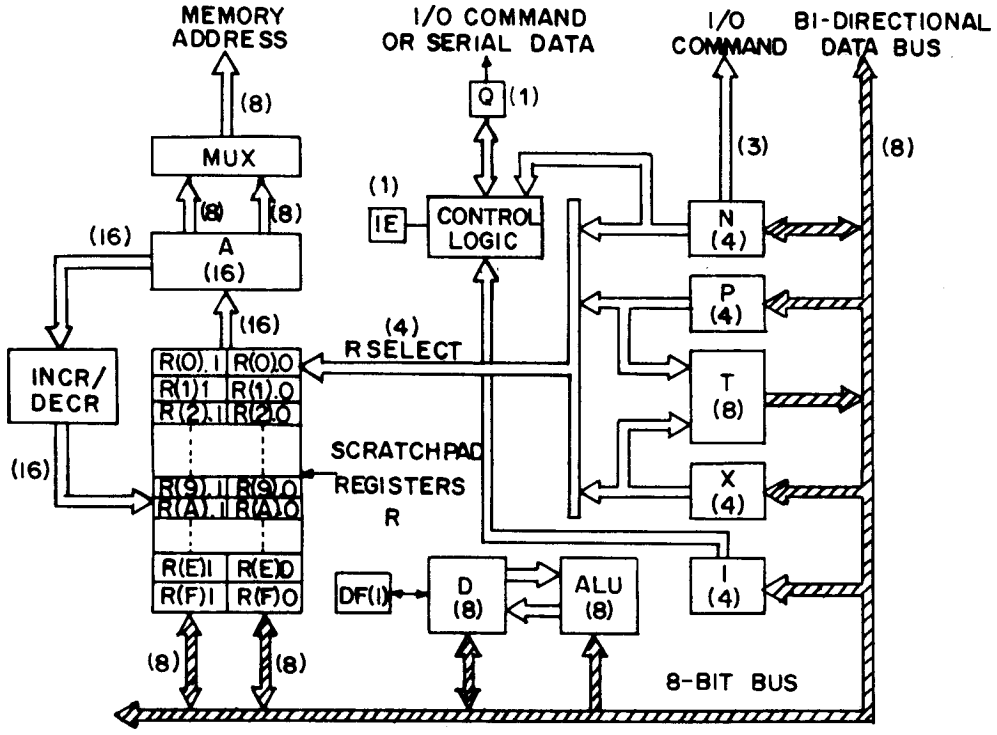

FIG. A 5.1 (b) Internal structure of the CDP 1802 Microprocessor.

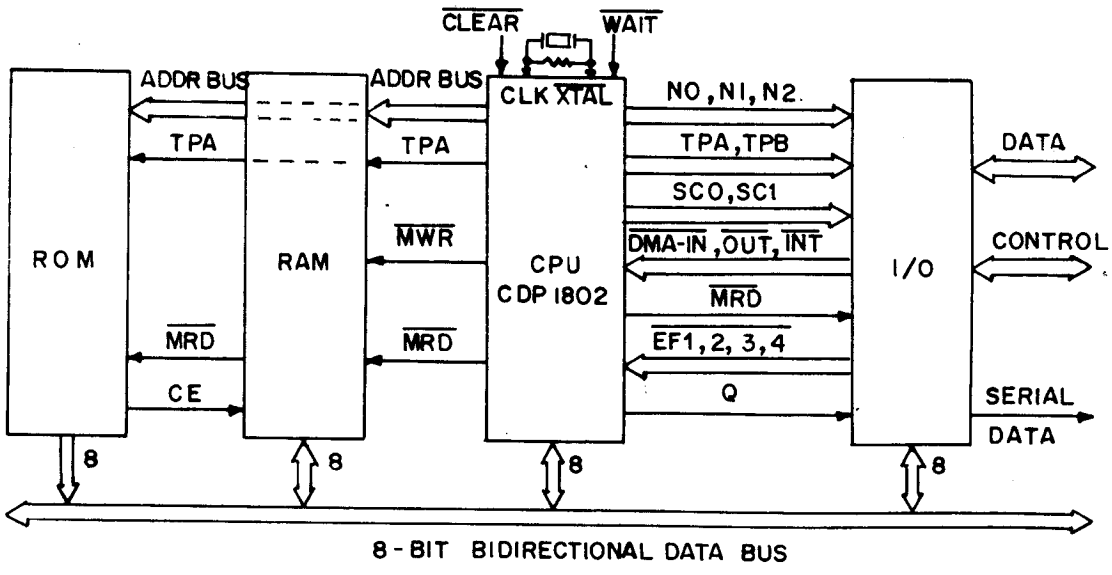

FIG. A5.1(c). Block diagram of typical computer system using the RCA COSMAC Microprocessor CDP 1802.

Fig. A5.2(a), (b), (c) and (d) give the timing diagrams for executing various instructions.

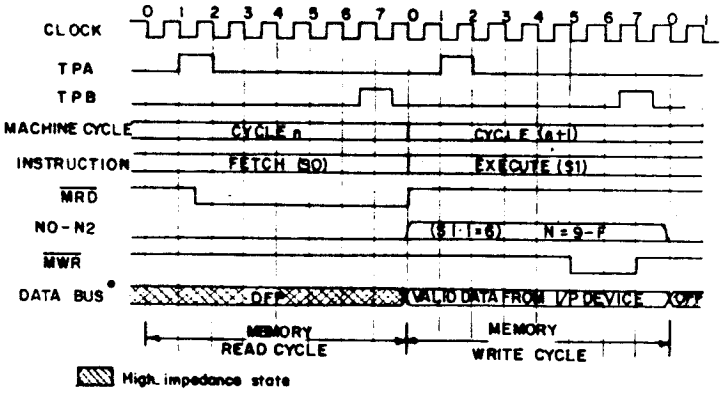

FIG. A 5.2 (a) Input instruction timing.

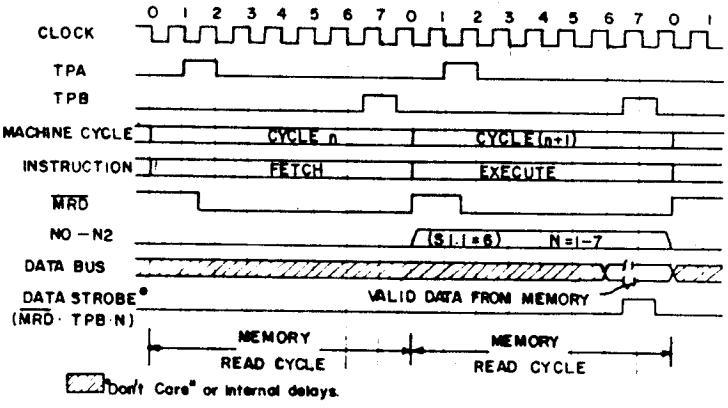

FIG. A 5.2b Output instruction timing.

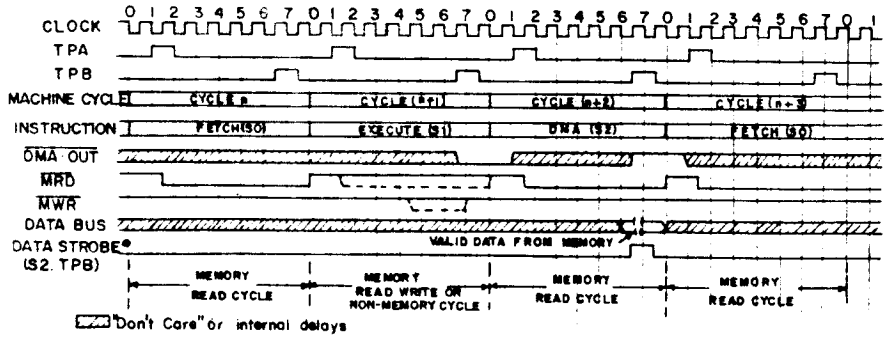

FIG. A 5.2 (c) DMA-OUT timing.

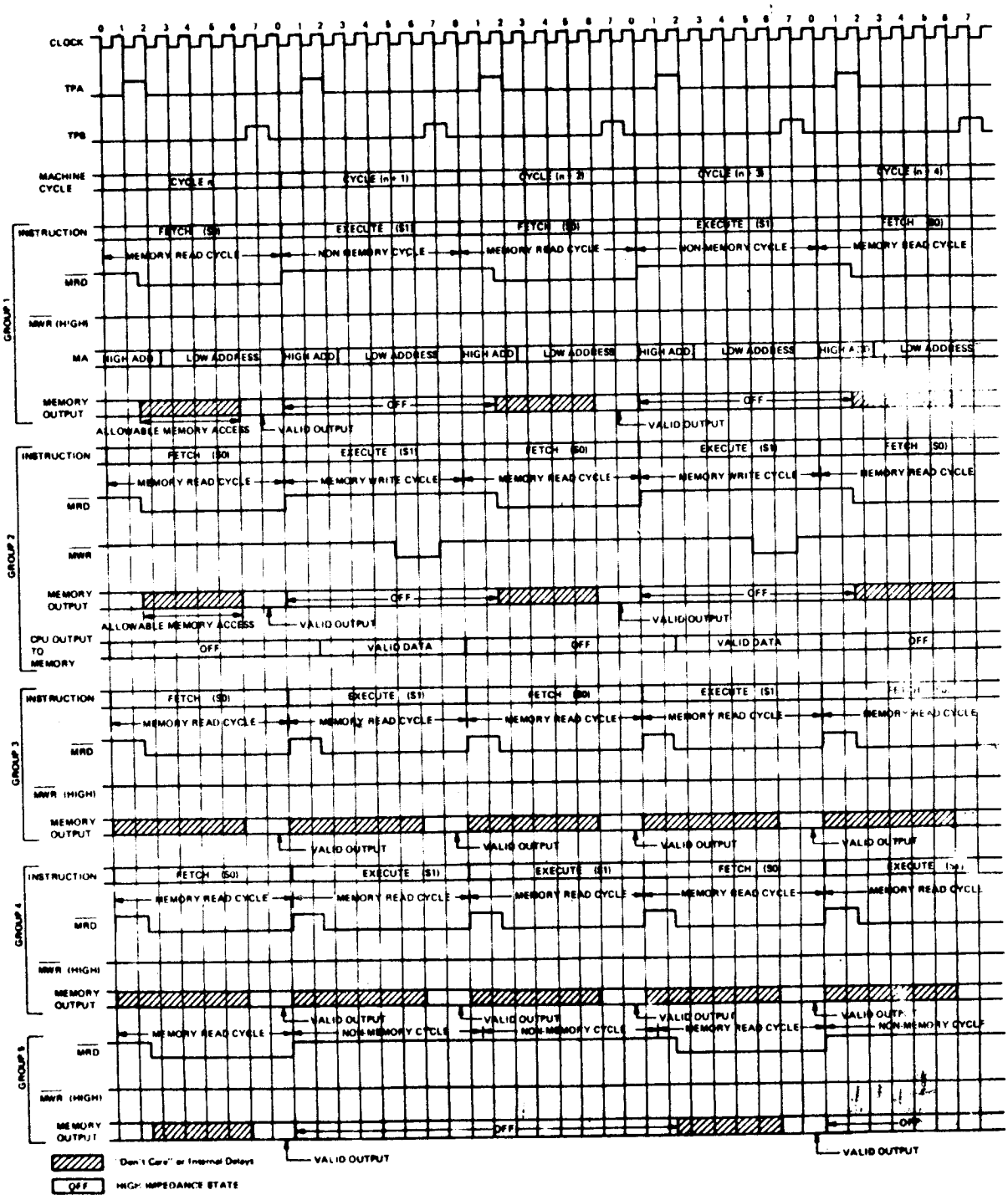

FIG. A5.2(d)– *Instruction set timing.*

APPENDIX - 6

TYPICAL SETTING FOR POST-INTEGRATION MULTIPLIER

Consider an example with Console Settings as:

BEAM START, BS_B = 200

BEAM FINISH, BF_B = 300

Pre-integration time = 256 ms

The total time for data processing and transferring the same to MTU is calculated as below :

Time for processing = (100x0.256) ms for 100 beams + (256x0.006) for phase correction

= 27.14 ms

Time for transferring on MTU operating at 500 Hz = (100 x 4) ms = 400 ms

Therefore, minimum time required between successive transfer of data onto MTU = (400 + 27.14) = 427.14 ms.

Hence, minimum post-integration multiplier of 2 will suffice.

APPENDIX - 7

DETAILS OF VIDEO RAM MATROX TYPE-MTX 1632 SL

The MTX-1632SL is a TV CRT controller designed for use in systems that require display of alphanumeric data. On the input side the device is connected to bus organized systems and looks like a 512 X 8 RAM. The output is a video signal which directly drives a TV monitor to provide a 16 X 32 field of 512 ASCII characters.

Fig. A7.1 is the block diagram of the Video RAM and Fig. A7.2 shows the internal circuitry of the RAM. Fig. A7.3 gives the timing diagrams for read and write cycles of the RAM.

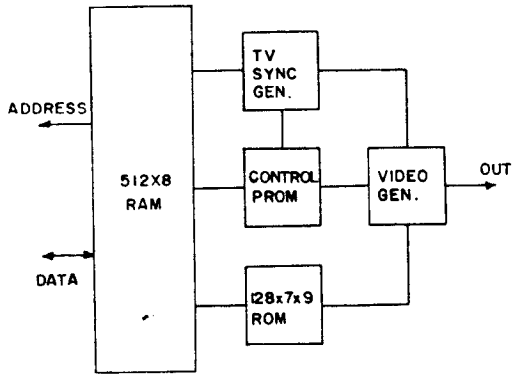

FIG. A 7.1 MTX-1632 VIDEO RAM BLOCK DIAGRAM.

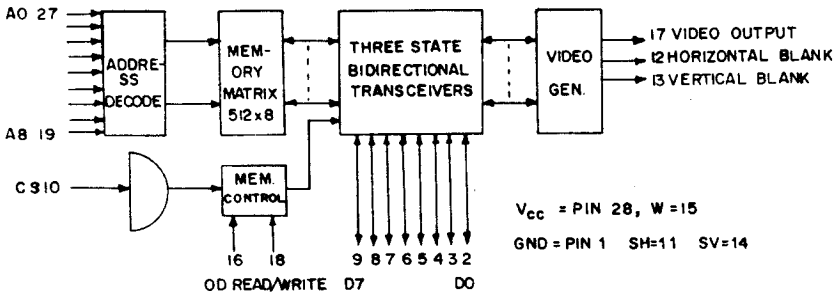

FIG. A 7.2 BLOCK DIAGRAM.

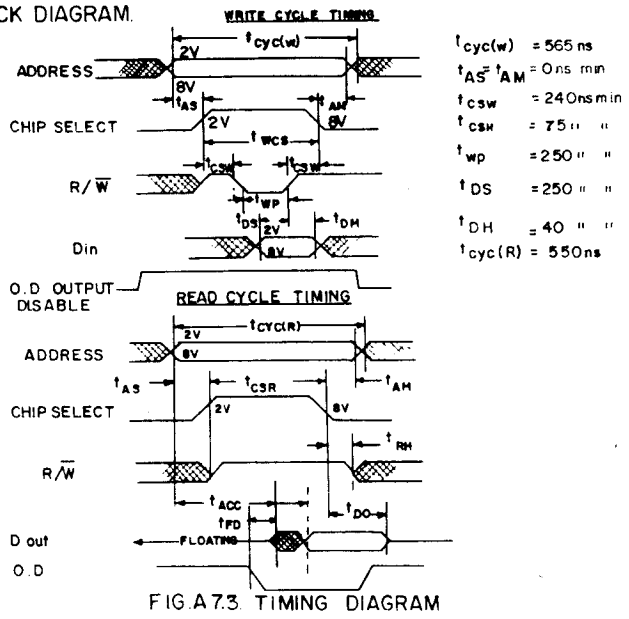

FIG. A 7.3. TIMING DIAGRAM

APPENDIX - 8

DETAILS OF GRAPHICS MODULE MATROX TYPE MTX-256

The MTX-256 is a modular unit designed for graphics applications. On the input side the device looks like a 4 location X 8 bit static random access memory (write only). Two memory locations (1, 2) are used for X and Y coordinates (8 bits each). Location address 4 is used for writing data (intensity) of the X, Y addressed dot into the refresh memory. Writing into address 3 will load simultaneously all 65,536 dot locations with 0 or 1. This mode can be used to clear the screen. All the timing and the data signals are the same as for any other RAM in the microcomputer address space.

The output is a composite video signal which directly drives commercial TV monitors to provide a 256 X 256 dot raster. Vertical and horizontal synchronous pulses are also provided as separate outputs. They can be used to drive the MTX-1632 SL alphanumeric module. Mixing both video signals will provide a fully graphic/alphanumeric display.

Fig. A8.1 gives the block schematic of the graphics module. Fig. A8.2 gives the input/output signals for the module. Fig. A8.3 and A8.4 give cursor format and cursor vector control. Fig. A8.5 is the typical connection with the Video RAM. Fig. A8.6 gives the timing diagram of the write cycle.

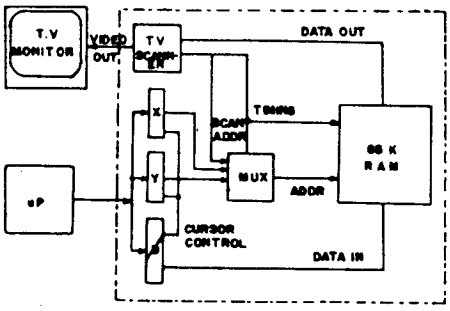

FIG.A8.1 BLOCK DIAGRAM.

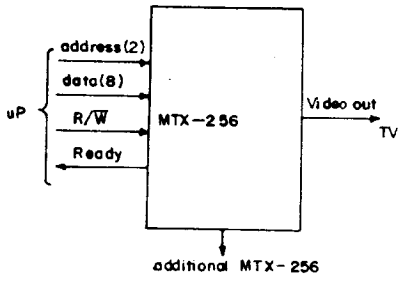

FIG. A8.2 SIGNALS.

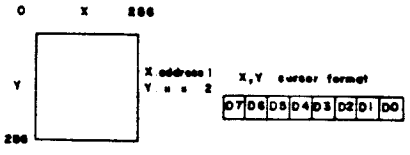

FIG.A 8.3 CONTROL WORD FORMAT.

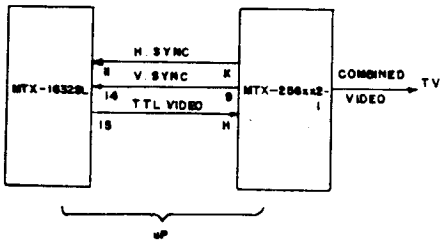

FIG. A8.5 INTERCONNECTION.

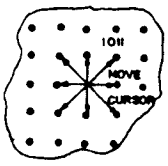

	D7	D6	D5	D4	CURSOR MOVES.
0	0	0	0	0	• (STAY)
1	0	0	0	1	→
2	0	0	1	0	↓
3	0	0	1	1	↘
4	0	1	0	0	•
5	0	1	0	1	←
6	0	1	1	0	↑
7	0	1	1	1	↖
8	1	0	0	0	•
9	1	0	0	1	→
10	1	0	1	0	↑
11	1	0	1	1	↗
12	1	1	0	0	•
13	1	1	0	1	←
14	1	1	1	0	↓
15	1	1	1	1	↘

FIG.A 8.4 CURSOR MOVEMENT.

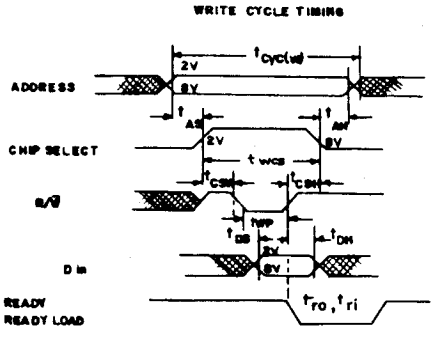

RECOMMENDED AC OPERATING CONDITIONS

PARAMETER	SYMBOL	MIN.	UNIT
Address set up Time	t_{AS}	0	ns
Address Hold Time	t_{AH}	0	ns

FIG. A8.6 TIMING DIAGRAM.

FIG.A 8.1.–A.8.6 DETAILS OF THE GRAPHICS MODULE.

REFERENCES

1. ALLEN L.R., PALMER H.P., and ROWSON B., Nature, 188, 731, 1960.

2. ALFVEN H. and HERLOFSON H., Cosmic radiation and radio stars, Physical Review, 78, 616, 1950.

3. ANDERSON B., DONALDSON W., PALMER H.P., and ROWSON B., Observations of quasi-stellar and other radio sources with an interferometer of resolving power 0.4 sec of arc, Nature, 205, 375-376, 1965.

4. BAADE W and MINKOWSKI R., Identification for the radio sources in Cassiopeia, Cygnus A and Puppis A, Astrophys. Journal, 119, 206, 1954.

5. BLAKE D.H., CRUTCHER R.M. and WATSON W.D., Identification of the anomalous 26.131-MHz nitrogen line observed towards Cas A, Nature, 287, Oct. 1980.

6. BLUM E.J., Sensibilite des radiotelescopes et recepteurs a Correlation, Ann. Astrophysics, 22, 140-163, 1959.

7. BLYTHE J.H., A new type of pencil beam aerial for radio astronomy, Monthly Notices Roy. Ast. Soc. 117, 644-651, 1957.

8. BOLTON J.G. and STANLEY G.J., Observations on the variable source, radio-frequency radiation in the Constellation Cygnus, Australian J. Scientific Research, Ser.A, 1, 58, 1948.

9. BOS A., Final Proposal for 10240 channel digital correlator for Culgoora radio heliograph, CSIRO-Division of Radio Physics, Int. Report, 1979.

10. BOS A., RAIMOND ERNST and VAN SOMEREN GREVE H.W., A Digital spectrometer for the Westerbork Synthesis radio telescope, Netherlands Foundation of Radio Astronomy, Preprint Nov. 1980.

11. CASSE J.L. and MULLER C.A., The synthesis radio telescope at Westerbork, the 21 cm continuum receiver system, Astronomy and Astrophysics, 31, 333-338, 1974.

12. CHRISTIANSEN W.N. and WELLINGTON K.J., A new radio telescope of 40 sec. of arc resolving power for southern sky observations, Nature, 209, 1173-76, March 1966.

13. CHRISTIANSEN W.N. and HOGBOM J.A., Radio telescopes, Cambridge University Press, 1969.

14. CLARK B.G., An interferometer investigation of the 21cm hydrogen line absorption; Calif. Inst. Tech. Radio Obs. Report, 6, 1965.

15. CLARK B.G., Digital processing methods for aperture synthesis observations, Proc. Image Formation from Coherence functions in Astronomy, IAU Colloquium, 49, 1979.

16. COLE T., Finite sample correlations of quantised gaussians, Australian Journal of Physics, 21, 273-282, 1968.

17. COOPER B.F.C., Correlation with two bit quantisation, Australian Journal of Physics, 23, 521-527, 1970.

18. COOPER B.F.C., ABLES J.G., et al, 1024 channel digital correlator, An internal report CSIRO, Sept. 1970.

19. DICKE R.H., The measurement of thermal radiation at microwave frequencies, Rev. of Sci. Instr., 17, 268-275, July 1946.

20. ERICKSON W.C., A proposal for operation of the Clark Lake Radio Telescope, An internal report, University of Maryland, May 1975.

21. EWEN H.I. and PURCELL E.M., Radiation from galactic Hydrogen at 1420 Mc/s, Nature, 168, 356-357, Sep. 1951.

22. FINLAY E.A. and JONES B.B., Measurements of Source strengths at 29.9 MHz, Australian Journal of Physics, 26, 389-402, 1973.

23. FISHER J. RICHARD., Design tests of the fully steerable wideband decametric array at Clark Lake Radio Observatory, Ph.D. thesis, University of Maryland, 1972.

24. FOMALONT EDWARD B., Fundamentals and deficiencies of aperture synthesis, Proc. Image formation from Coherence functions in astronomy, IAU colloquium, 49, 1979.

25. FRATER R.H. and SKELLERN D.J., Direct transform hardware processing of rotational Synthesis data-1 Astron. Astrophys., 68, 391-396, 1978.

26. FRATER R.H., Direct transform hardware processing of rotational synthesis data-2, Astron. Astrophys. 68, 397-403, 1978.

27. FRATER R.H., The two dimensional representation of three-dimensional interferometer measurements, Proc. Image Formation from Coherence functions in Astronomy, IAU Colloquium, 49, 1979.

28. GREENSTEIN J.L. and MATTHEWS T.A., Redshift of the unusual radio source 3C-48, Nature, 197, 1041, 1963.

29. HAGEN J.P and Mc CLAIN E.F., Galactic absorption of radio waves, Astrophys. Journal, 120, 368-370, Sept. 1954.

30. HAZARD C., MACKEY M.B. and SHIMMINS A.J., Investigation of the radio source 3C273 by the method of linear occultations, Nature, 197, 1037, 1963.

31. HEWISH A., SCOTT P.F. and WILLE D., Interplanetary Scintillations of small diameter radio sources, Nature, 203, 1214-1217, Sep. 1964.

32. HEWISH A., BELL S. JOCELYN., PILKINGTON J.D.H., SCOTT P.F. and COLLINS R.A., Observation of rapidly pulsating radio source, Nature, 217, 709-713, Feb. 1968.

33. HEY J.S., PHILIPS J.W., PARSONS S.J., Cosmic radiations at 5 metres wavelength, Nature, 157, 296-297, Mar. 1946(a).

34. HEY J.S., PHILIPS J.W., PARSONS S.J., Fluctuations in Cosmic radiations at radio frequencies, Nature, 158, 234, Aug. 1946(b).

35. HINDER RICHARD and RYLE M., Atmospheric limitations to the angular resolution of aperture synthesis radio telescopes, Monthly Not. Roy. Ast. Soc., 154, 229-253, 1971.

36. HOGBOM J.A. and BROUW W.N., The synthesis radio telescope at Westerbork, Principles of operation, performance and data reduction, Astronomy and Astrophysics, 33, 289-301, 1974.

37. JANSKY K.G., Directional Studies of Atmospherics at high frequencies, Proc. IRE, 20, 1920-1932, Dec. 1932.

38. JANSKY K.G., Electrical disturbances apparently of extra-terrestrial origin, Proc. IRE, 21, 1387-1398, Oct. 1933.

39. JANSKY K.G., A note on the interstellar interference, Proc. IRE, 23, 1158-1163, Oct. 1935.

40. JONES BEVAN., An aperture synthesis survey at 30 MHz, Ph.D. thesis, University of Sydney, Jan. 1973.

41. KENDERDINE S., Fourier Transform supersynthesis, Astronomy and Astrophysics Suppl., 15, 413-415, 1974.

42. KIEPENHEUER K.O., Cosmic rays as the source of general galactic radiation, Physics Review, 79, 738, 1950.

43. KLINGLER ROLF JERG., Quantisation noise of signal correlators, M.Sc. thesis, University of British Columbia, May 1972.

44. KONOVALENKO A.A. and SODIN L.G., Neutral ^{14}N in the interstellar medium, Nature, 283, 360-364, Oct. 1980.

45. KRAUS JOHN D., Radio Astronomy, McGraw Hill Co., 1966.

46. KULKARNI SHRINIVAS R. and HEILES CARL., How to obtain the true correlation from a 3 level digital correlator, An internal report, University of California, USA.

47. LITTLE L.T. and HEWISH A., Interplanetary Scintillations and its relation to angular structure of radio sources, Monthly Not. Roy. Ast. Soc., 134, 221-237, 1966.

48. MANCHESTER R.N., Radio timing observations, IAU Symposium on pulsars, 95, 267-276, Reidel Publication, 1980.

49. MATTHEWS T.A., MORGAN W.W., and SCHMIDT M., A discussion of galaxies identified with radio sources, Astrophys. Journal, 140, 35, 1964.

50. MILLS B.Y. and LITTLE A.G., A high resolution aerial system of a new type, Aust.Journal of Physics, 6, 272-278, 1953.

51. MILLS B.Y., Cross type radio telescope, Proc. IRE Australia, 24, 132-140, Feb. 1963.

52. MILLS B.Y., AITCHISON R.E., LITTLE A.G., and Mc ADAM W.B., The Sydney University cross-type radio telescope, Proc. IRE Australia, 24, 156-165, Feb. 1963.

53. MULLER C.A. and OORT J.H., The Interstellar Hydrogen line at 1420 Mc/s and an estimate of galactic rotation, Nature, 168, 357-358, 1951.

54. O' SULLIVAN J.D., Distribution of digitising noise in digital cross-correlation spectra, Addendum to Dwingeloo Internal Report, ITR 139, May 1980.

55. PENZIAS A.A. and WILSON R.W., A measurement of excess antenna temperature at 4080 Mc/S, Astrophys. Journal, 142, 419-421, 1965.

56. RADHAKRISHNAN V., Fifteen months of pulsar astronomy, Proc. Astron. Soc. Aust., 1, 254-263, Sep. 1969.

57. RADHAKRISHNAN V., BROOKS J.W., etal, The Parkes Survey of 21 cm Absorption in discrete source spectra, Parkes hydrogen line interferometer., The Astrophys. J. Suppl. Series, 24, 1-14, 1972.

58. READ R.B., Accurate measurement of the declinations of radio sources, Astrophys. Journal, 138, 1-29, July 1963.

59. REBER G., Cosmic Static, Astrophys. Journal, 91, 621-624, June 1940 (a).

60. REBER G., Cosmic Static, Proc. IRE, 28, 68-70, Feb. 1940 (b).

61. REBER G., Cosmic Static, Proc. IRE, 30, 367-378, Aug. 1942.

62. REBER G., Cosmic Static, Astrophys. Journal, 100, 279-287, Nov. 1944.

63. REBER G., Cosmic Static, Proc. IRE, 36, 1215-1218, Oct. 1948.

64. REDHEAD A.C.S. and WILKINSON P.N., The mapping of compact radio sources from VLBI data, The Astrophys. Journal, 223, 25-36, July 1978.

65. REDHEAD A.C.S., VLBI mapping of the nuclei of radio galaxies and quasars, IAU Symposium, No. 92, Aug. 1979.

66. RYLE M., A new radio interferometer and its applications to the observations of weak radio stars, Proc. Royal Society London., Ser.A, 211, 351-375, 1952.

67. RYLE M., HEWISH A., and SHAKESHAFT J.R., The synthesis of large radio telescopes by the use of radio interferometer, IRE Trans. on antennas and Prop., AP-7, Suppl. S120-124, 1959.

68. RYLE M. and HEWISH A., The synthesis of large radio telescopes, Monthly Notices Roy. Ast. Soc., 120, 220-230, 1960.

69. SCHMIDT M., 3C273: A star like object with a large redshift, Nature, 197, 1040, 1963.

70. SHKLOVSKY I.S., Secular variations of the flux and intensity of radio emission from discrete radio sources, Soviet Astronomical AJ., 4, 243, 1960.

71. SMITH F.G., An accurate determination of the positions of four radio stars, Nature, 168, 555, 1951.

72. VAN DE HULST H.C., Radio waves from Space, Ned. Tijdschr. Natuurk, 11, 201-221, 1945.

73. VAN SOMEREN GREVE H.W., The data handling of Westerbork Synthesis radio telescope, Astronomy and Astrophysics Suppl., 15, 343-352, 1974.

74. WEINREB S., A digital spectral analysis technique and its application to radio astronomy, Ph.D. thesis, MIT, USA, Aug. 1963.